Machine Learning of Functional Magnetic Resonance Imaging Network Connectivity Predicts Substance Abuse Treatment Completion

Supplemental Information

Supplemental Methods

Participants

Over the term of the project, 467 participants (208 men, 259 women) completed informed consent and were screened for study inclusion. Of 467 participants screened, 257 met the criteria for enrollment (121 men, 136 women). All 257 participants completed functional Magnetic Resonance Imaging (fMRI) data collection, though 118 were not selected for final analysis (n = 139) because: they were on antipsychotic medication (n = 3), anticipated a release or transfer from the facility in less time than would allow for the completion of the protocol (n = 30), had a family history of psychosis (n = 2), had an IQ below 70 (n = 1), had scheduling conflicts (n = 4), had an artifact and could not be used in final fMRI data analysis (n = 1), did not meet diagnostic criteria for cocaine, heroin, or methamphetamine dependence, or had abstained from substance use for longer than three months prior to incarceration (n = 32), were diagnosed with psychosis (n = 2), had less than a sixth grade reading level (n = 4), opted not to participate following the consent (n = 9), were diagnosed with schizophrenia (n = 1), were in segregation (n = 1), sought other drug treatment (n = 11), had significant movement of greater than 1.5 mm translation and 1.5 degrees of rotation during fMRI data collection (n =12), poor behavioral performance (n = 3), performing only one run of the Go/NoGo fMRI task (n = 1), or had a history of significant traumatic brain injury (n = 1).

Two-hundred ten did not meet study eligibility criteria because: they absconded (n = 1), were over the age of 55 (n = 1), anticipated a release or transfer from the facility in less time than would allow for the completion of the protocol (n = 23), were on antipsychotic medication (n = 13), had a family history of psychosis (n = 9), had scheduling conflicts (n = 2), were MRI incompatible (n = 42), did not meet diagnostic criteria for cocaine, heroin, or methamphetamine dependence, or had abstained from substance use for longer than three months prior to incarceration (n = 38), opted not to participate following the consent (n = 13), were diagnosed with psychosis (n = 13), had less than a sixth-grade reading level (n = 23), sought other drug treatment (n = 4), were clinically unstable (i.e., report current or recent suicidal ideation) (n = 7), or had a history of significant traumatic brain injury (n = 5). Exclusion data were unavailable for n = 16 participants. Of the participants completing informed consent and screening for the study, 225 (98 males, 127 females) were assigned to one of three therapy cells using a pseudorandom process. A total of 151 participants (59 males, 93 females) completed the entire therapy protocol (nine or more sessions).

Procedures and Ethical Considerations

Initial contact was made with potential study participants through announcements by research staff at the correctional facilities. Meetings were scheduled with interested participants and informed consent was obtained. Participants were informed of their right to discontinue participation at any point and that their participation was in no way associated with their status at the facility, their parole status, and there were no direct institutional benefits. Participants were paid at the rate of the hourly wage at the facility. All procedures were approved by the Human Research Review Committee at the research institution and correctional facilities where the study was conducted.

Assessment Measures

Depressive symptomatology. Depressive symptomatology was assessed using the Beck Depression Inventory-II (BDI-II) (1), a 21-item self-report measure that assesses the severity of depressive symptoms. Depressive symptom measures were unavailable for five participants. The Cronbach's alpha for the BDI-II in this sample was .90.

Anxiety symptomatology. Anxiety symptomatology was assessed using the State-Trait Anxiety Inventory (STAI) (2), a 40-item measure that assesses the intensity of anxiety symptoms and distinguishes between state anxiety and trait anxiety. Anxiety symptoms were unavailable for eighteen participants. The Cronbach's alpha for the STAI in this sample was .72.

Psychopathy. Psychopathy was assessed using the PCL-R (3, 4), comprising two factors; Factor 1 assessing callous interpersonal and affective traits, and Factor 2 assessing impulsive lifestyle and antisocial behavior. In the current study, Factor 2 was used as an index of impulsivity. Factor 1 and 2 scores were unavailable for 31 participants. The Cronbach's alpha for the PCL-R in this sample was .77.

Motivation for change. Motivation for change was assessed using the University of Rhode Island Change Assessment (URICA (5)), a continuous measure of four stages of how a person may feel about making changes before they acknowledge they have a problem (precontemplation), after they acknowledge they have a problem (contemplation), once they take steps toward treatment (action), and maintaining the change (maintenance). URICA scores were unavailable for 15 participants. The Cronbach's alpha for the URICA in this sample was .80.

Estimated IQ. IQ was estimated using the Vocabulary and Matrix Reasoning subtests of the Wechsler Adult Intelligence Scale (6) (mean = 96.07, SD = 11.27). IQ scores were unavailable for four participants.

Years of Substance Use. Years of regular substance use were measured using a modified version of the Addiction Severity Index (ASI-X (7)) by calculating the cumulative years of regular use (i.e., three or more times per week for a minimum of one month) for all substances (alcohol, heroin, cocaine, methamphetamine, cannabis, hallucinogens, and inhalants) combined. Total scores were then divided by participant's age to control for opportunity to use. ASI scores were unavailable for 10 participants. The Cronbach's alpha for the ASI in this sample was .77.

Experimental Go/NoGo Task

Participants then performed a difficult, previously published Go/NoGo paradigm (8) containing two experimental runs, each comprising 245 visual stimuli, presented to participants using the computer-controlled visual presentation software package, Presentation. Each stimulus appeared for 250 ms in white text within a continuously displayed rectangular fixation box. Participants were instructed to respond as "quickly and accurately as possible" with their right index finger every time the target ("Go") stimulus (a white "X") appeared, and to withhold a response when the distracter "No/Go" stimuli (a white "K") appeared. Targets appeared with higher frequency (84%, 412 trials with 206 for each run) than distractors (16%, 78 trials with 39 for each run) to establish a strong stimulus-response mapping on "Go" trials. Two K's were never presented sequentially. The stimuli were approximately 3 x 5 visual degrees, and were presented for 250 ms on a black background. The interstimulus interval was pseudo-randomly jittered (1-3 s stimulus-onset asynchrony (SOA; 9); averaging 1.5 s). Prior to recording, each participant performed a block of 10 practice trials to ensure that the instructions were clearly understood. The SOA between Go stimuli varied to the constraint that three Go stimuli were presented within each consecutive 6 s period. The NoGo stimuli were interspersed among the Go stimuli in a pseudorandom manner subject to two constraints: the minimum SOA between a Go

and NoGo stimulus was 1000 ms; the SOA between successive NoGo stimuli was in the range eight to 14 s.

Analysis of Functional Magnetic Resonance Imaging Data

A mean functional image volume was constructed for each run from the realigned image volumes. The mean EPI image from each run was normalized to the EPI template. The spatial transformation into standard MNI space was determined using a tailored algorithm with both linear and nonlinear components (10). The normalization parameters determined for the mean functional volume were then applied to the corresponding functional image volumes for each participant. The normalized functional images were smoothed with a 6 mm full width at half-maximum (FWHM) Gaussian filter. Event-related responses were modeled using a synthetic hemodynamic response function composed of two gamma functions. The first gamma function modeled the hemodynamic response using a peak latency of 6 s. A term proportional to the derivative of this gamma function was included to allow for small variations in peak latency. The second gamma function and associated derivative was used to model the small "overshoot" of the hemodynamic response on recovery. A latency variation amplitude-correction method was used to provide a more accurate estimate of hemodynamic response for each condition that controlled for differences between slices in timing and variation across regions in the latency of the hemodynamic response (11). High-pass (cutoff period 116 s) and low-pass (cutoff period 0.23 s) filters were applied to remove any low- and high-frequency confounds, respectively. Condition-specific derivative terms (11) were extracted for analysis. SPM5 using MATLAB 2014a was used for these analyses.

The primary purpose of this study was to use functional network connectivity (FNC) features for classification of substance abuse treatment outcomes. Functional connectivity (FC) is

defined as the correlation (or other kinds of statistical dependency) among spatially remote brain regions (12). FC analysis documents interactions among brain regions either during tasks or during rest. Two widely used FC approaches are: (a) seed-based analysis (13-18) and (b) spatial Independent Component Analysis (ICA) (19-23). ICA is a data-driven multivariate analysis method that identifies distinct groups of brain regions with the same temporal pattern of hemodynamic signal change. In the seed-based approach, individual seed voxels from predefined brain regions of interest (ROI) are chosen and the cross correlation of other voxels' time courses (TCs) with the selected seeds then computed, to derive a correlation map. This map is then thresholded to identify voxels with significant FC with the seed voxels.

An alternative approach is based on ICA, a blind source separation method can recover a set of signals from their linear mixtures. This method has yielded fruitful results with fMRI data (24, 25). ICA estimates maximally independent components using independence measures based on higher-order statistics. Compared to general linear model approaches, ICA requires no specific temporal model (task-based design matrix), making it ideal for analyzing resting-state data (26). Depending on the data matrix formation, one can perform either temporal (tICA) or spatial ICA (sICA) on fMRI data with sICA most commonly used (19, 20, 27). sICA decomposes fMRI data into a set of maximally spatially independent maps and their corresponding time-courses. Each thresholded sICA map may consist of several remote brain regions forming a brain functional network. sICA generates consistent spatial maps while modeling complex fMRI data collected during a task or in a resting-state (28) although the task can result in a subtle modulation of the spatial patterns (29). The dynamics of the BOLD signal within a single component is described by that component's TC. Regions contributing significantly within a given component are strongly functionally connected to each other.

Group ICA was performed on the preprocessed fMRI time-series data (20). These methods were implemented in the MATLAB toolbox for ICA of fMRI (GIFT) and have been detailed previously (20, 25). A two-stage PCA data reduction step was implemented, at the single subject level 150 PCs were extracted, followed by a group PCA step using 75 components, lower than the first step (30). The number of ICA components was selected in light of evidence that a high number (70-100) of independent components consistently and stably estimate data (31-34). The data reduction was followed by a group sICA, performed on the participants' aggregate data, resulting in the final estimation of our ICs. The algorithm used in this process was the infomax algorithm, which attempts to minimize the mutual information of network outputs (35). This was followed by a back reconstruction of single-subject time courses and spatial maps from the raw data using the group solution to accurately depict the participant-to-participant variability that existed in the data (30). The resulting single-subject time-course amplitudes were then intensity prenormalized (20). These spatial maps and TCs were then regressed against the same design matrix used in the SPM analysis. Spatial maps were reconstructed and converted to Z-values for each participant. Partial correlations were used to identify 34 non-artifactual components (Figures S1-S5) that were task related (Table S2). Non-artifactual components are expected to have peak activation in the gray matter and have low spatial overlap with known ventricles, vascular, motion, and susceptibility artifacts.

The FNC (36) among ICA TCs across the entire task were computed using Pearson correlation coefficients. These coefficients were used in support vector machine (SVM) models predicting which individuals would or would not complete treatment. Reducing dimensionality of the FNC features used in the models was crucial considering the current dataset would be considered small compared to the number of features in the context of machine learning. We

used double input symmetric relevance (DISR) (37) feature selection method. DISR is a fast filtering method designed to select a feature set that exhibits maximal mutual information with class labels while minimizing the mutual information among the selected features. This method reduced the feature set for each classification run from 561 to 50 for each participant during the cross-validation step. Frequency of selection for each variable was tracked to assess the relative usefulness of each feature in the prediction models.

The accuracy of these SVM models was confirmed with permutation tests. These tests were calculated by randomizing the labels (i.e., group membership as completed treatment or discontinued treatment prematurely) 1000 times and calculating classification measures within each iteration. When randomizing the labels, the ratio of classes constant was held constant. By calculating the proportion of times (of the 1000 iterations) where the measures were greater than our original classification measures, *p*-values reflecting the stability of our classification models were calculated.

Table S1. Descriptive Statistics and Independent Samples t-tests for Variables Used as Covariates

	All Participants (n=139)			Completed Group (n=107)			Discontinued Group (n=32)					
Variable	N	Mean	SD	N	Mean	SD	N	Mean	SD	t	df	p
Age	139	34.00	7.97	107	34.39	8.07	32	32.69	7.60	-1.06	137	.290
IQ	135	96.07	11.27	107	95.72	11.18	28	97.39	11.73	0.70	133	.486
Precontemplation	124	53.10	10.58	98	53.32	10.33	26	52.31	11.68	-0.43	122	.668
Contemplation	124	43.45	14.08	98	43.62	13.49	26	42.31	16.38	-0.42	122	.674
Action	124	50.97	11.75	98	51.07	12.02	26	50.58	10.89	-0.19	122	.850
Maintenance	124	47.98	10.78	98	48.37	9.22	26	46.54	15.48	-0.77	122	.444
State Anxiety	121	40.08	12.14	99	40.25	12.20	22	39.32	12.14	-0.33	119	.746
Trait Anxiety	121	43.21	11.27	99	43.36	11.61	22	42.50	9.84	-0.32	199	.747
Beck's Depression	134	16.37	10.98	107	16.56	11.54	27	15.63	8.49	-0.39	132	.695
PCL-R-F1	108	5.08	2.99	92	5.10	3.09	16	4.98	2.50	-0.14	106	.887
PCL-R-F2	108	12.70	3.23	92	12.74	3.27	16	12.48	3.10	-0.30	106	.768
Years of Sub. Use	139	1.29	0.62	103	1.27	0.64	26	1.39	0.55	0.86	127	.394

Note. All participants (n=139) either successfully completed or discontinued a cognitive behavioral substance abuse treatment program. Individuals in the completed group (n=107) include adult incarcerated offenders who successfully completed nine weeks of a cognitive behavioral substance abuse treatment program. Individuals in the discontinued group (n=32) include adult incarcerated offenders who discontinued treatment prior to nine weeks of a cognitive behavioral substance abuse treatment program. Assessments: Intelligence Quotient (IQ) was calculated from the Wechsler Adult Intelligence Scale III (WAIS-III); Precontemplation, Contemplation, Action, and Maintenance are summary scores of subscales from the University of Rhode Island Change Assessment (URICA); State Anxiety and Trait Anxiety are summary scores from the State and Trait Anxiety Questions from the State-Trait Anxiety Inventory (STAI); Beck's Depression is the total score from Beck's Depression Inventory (BDI-II); PCL-R-F1 and PCL-R-F2 are the Factor 1 and Factor 2 summary scores from the Psychopathy Checklist – Revised (PCL-R); Years of Sub. Use is the total number of years of substance use divided by participant's age was calculated by a modification of the Addiction Severity Index (ASI-X) divided by the participant's age.

Table S2. Summary of Independent Component Relationship to the Design Matrix

	Hits	**Correct Rejects**	**False Alarms**
Component	*t-value*	*t-value*	*t-value*
2	4.31***	1.40	3.87***
4	11.33***	2.24	3.72***
5	-25.70***	-16.48***	-0.29
6	6.66***	1.76	4.49***
7	-13.07***	-11.69***	-9.62***
9	5.54***	-0.56	-7.07***
12	13.43***	6.39***	0.52
16	-5.63***	-6.44***	-11.78***
21	5.25***	8.09***	-1.51
23	-13.19***	-1.76	-5.10***
31	10.80***	9.98***	-9.51***
32	-7.10***	0.63	-4.38***
34	-9.63***	-2.09	9.28***
38	-5.02***	-7.33***	12.42***
40	18.02***	17.82***	16.73***
41	2.76*	-1.44	3.78***
43	-16.74***	2.74*	-4.04***
44	1.62	0.50	4.45***
51	11.01***	5.79***	-1.11
54	12.84***	6.75***	3.96***
56	0.75	-7.38***	-4.21***
61	-3.52**	-10.54***	-2.24
62	5.17***	2.07	5.77***
63	3.55***	6.09***	14.64***
64	-7.44***	-6.42***	-11.23***
65	7.67***	14.51***	20.32***
66	4.51***	6.93***	3.92***
67	-2.35	-10.74***	-0.01
68	5.91***	15.70***	2.01
69	-12.65***	-12.33***	-1.88
70	-8.58***	-16.36***	-11.20***
71	-1.27	2.66	-1.86
73	-0.86	-2.25	-9.81***
74	5.53***	15.82***	0.05

Note. Relationship between time courses of independent components and the design matrix of experimental conditions Hits, Correct Rejections, and False Alarms are presented. A false-discovery rate correction for multiple comparisons was applied correction (38, 39).

*** $p < .001$

** $p < .005$

* $p < .01$

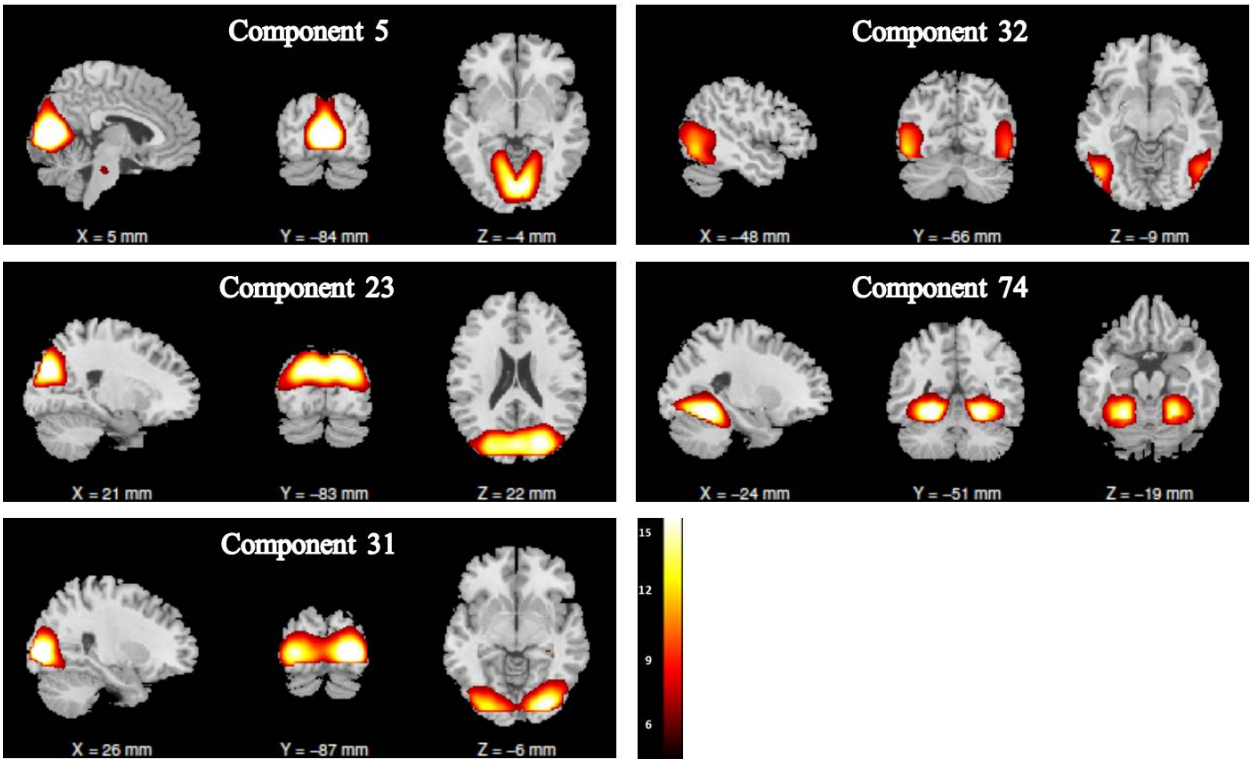

Figure S1. Spatial maps for five independent components in the occipital and cerebellar regions: Component 5 (cuneus); Component 23 (cuneus and cingulate gyrus); Component 31(middle occipital gyrus and thalamus); Component 32 (culmen and precuneus); Component 74 (inferior temporal gyrus).

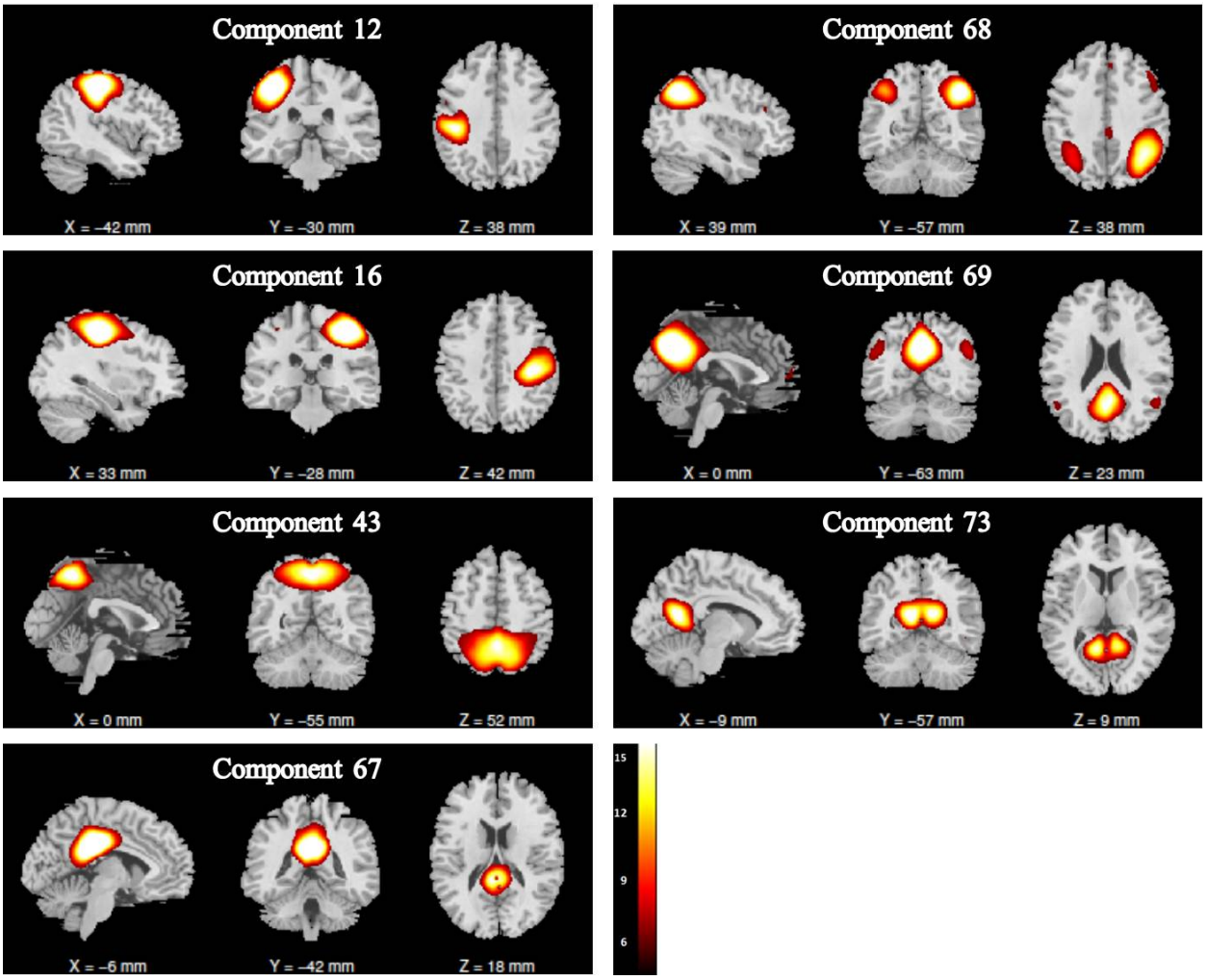

Figure S2. Spatial maps for seven independent components in posterior regions: Component 12 (postcentral gyrus, cingulate gyrus, and superior frontal gyrus); Component 16 (postcentral gyrus, cingulate gyrus, and claustrum); Component 43 (precuneus); Component 67 (cingulate gyrus); Component 68 (inferior parietal lobule, middle frontal gyrus, and middle frontal gyrus); Component 69 (precuneus, superior temporal gyrus, and parahippocampal gyrus); Component 73 (precuneus, fusiform gyrus, inferior parietal lobule, and thalamus).

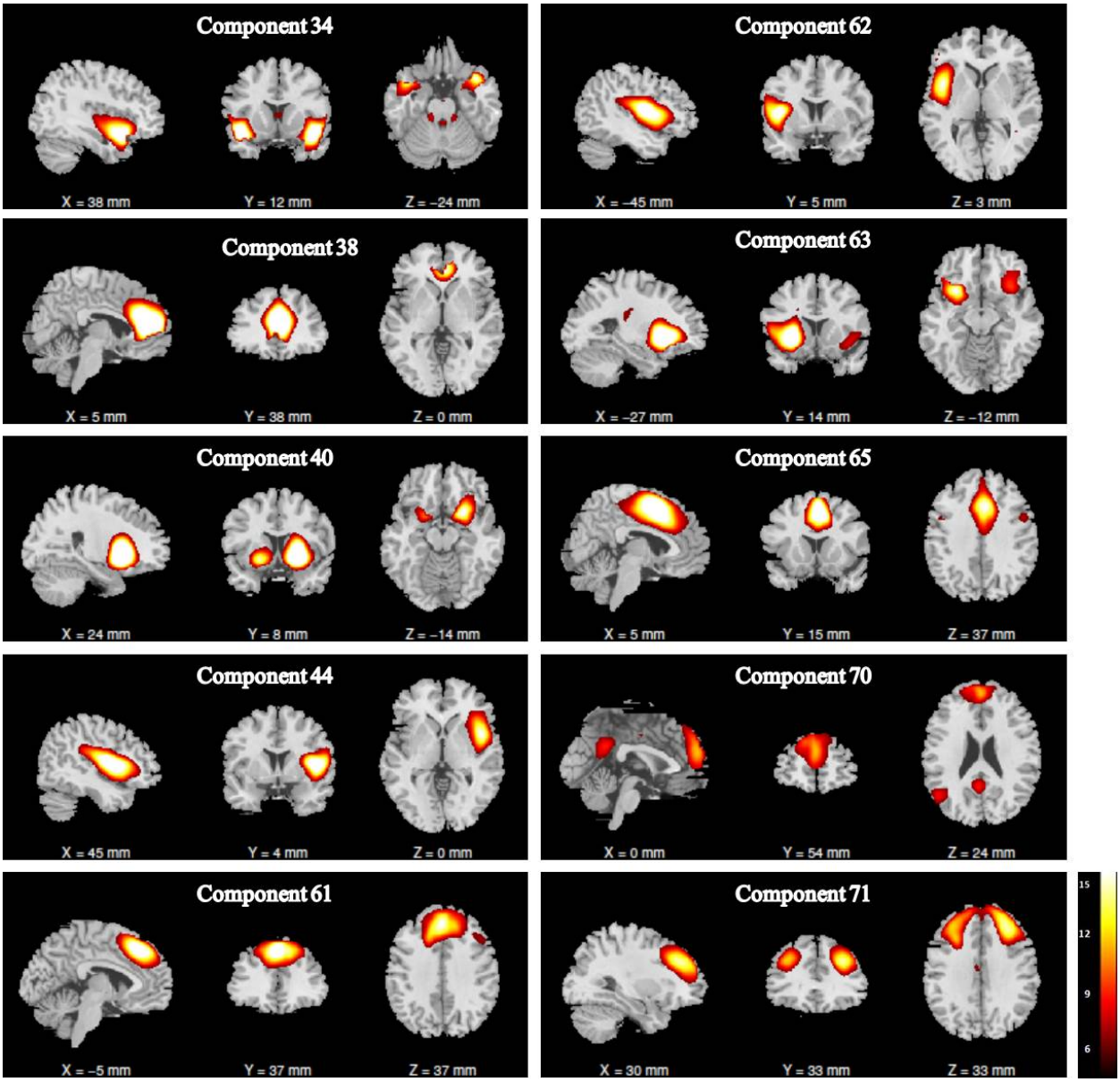

Figure S3. Spatial maps for ten independent components in frontal regions: Component 34 (superior temporal gyrus, culmen, and insula); Component 38 (rACC); Component 40 (Putamen, rACC); Component 44 (precentral gyrus, middle temporal gyrus, and middle frontal gyrus); Component 61 (middle frontal gyrus, caudate, and insula); Component 62 (left insula, hypothalamus, cingulate gyrus, and parahippocampal gyrus); Component 63(claustrum, inferior frontal gyrus, medial frontal gyrus); Component 65 (cACC); Component 70 (medial frontal gyrus, superior temporal gyrus, and putamen); Component 71 (superior frontal gyrus, cingulate gyrus, and precuneus).

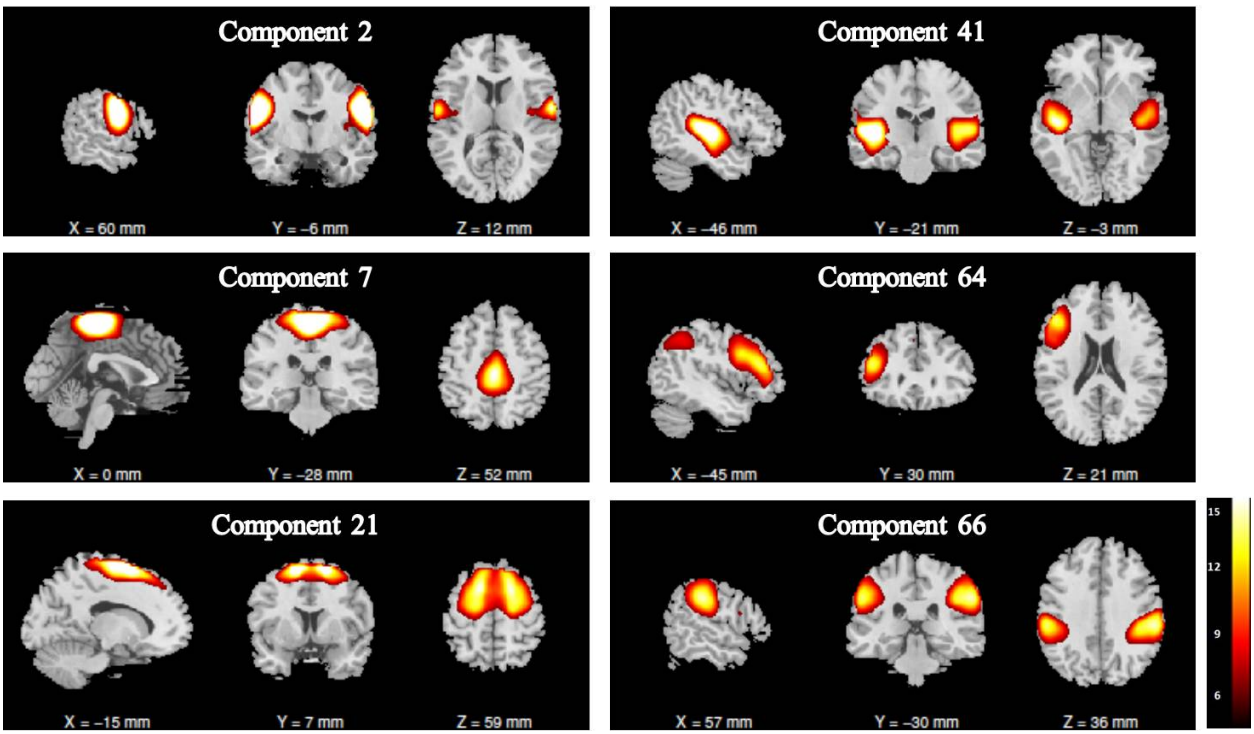

Figure S4. Spatial maps for six independent components accounting for motor, default mode network, and dorsal regions: Component 2 (precentral gyrus); Component 7 (middle frontal gyrus); Component 21 (superior frontal gyrus); Component 41 (superior temporal gyrus); Component 64 (middle frontal gyrus, superior parietal lobule, insula, inferior temporal gyrus); Component 66 (inferior parietal lobule, postcentral gyrus, sub-gyral, cuneus, and putamen).

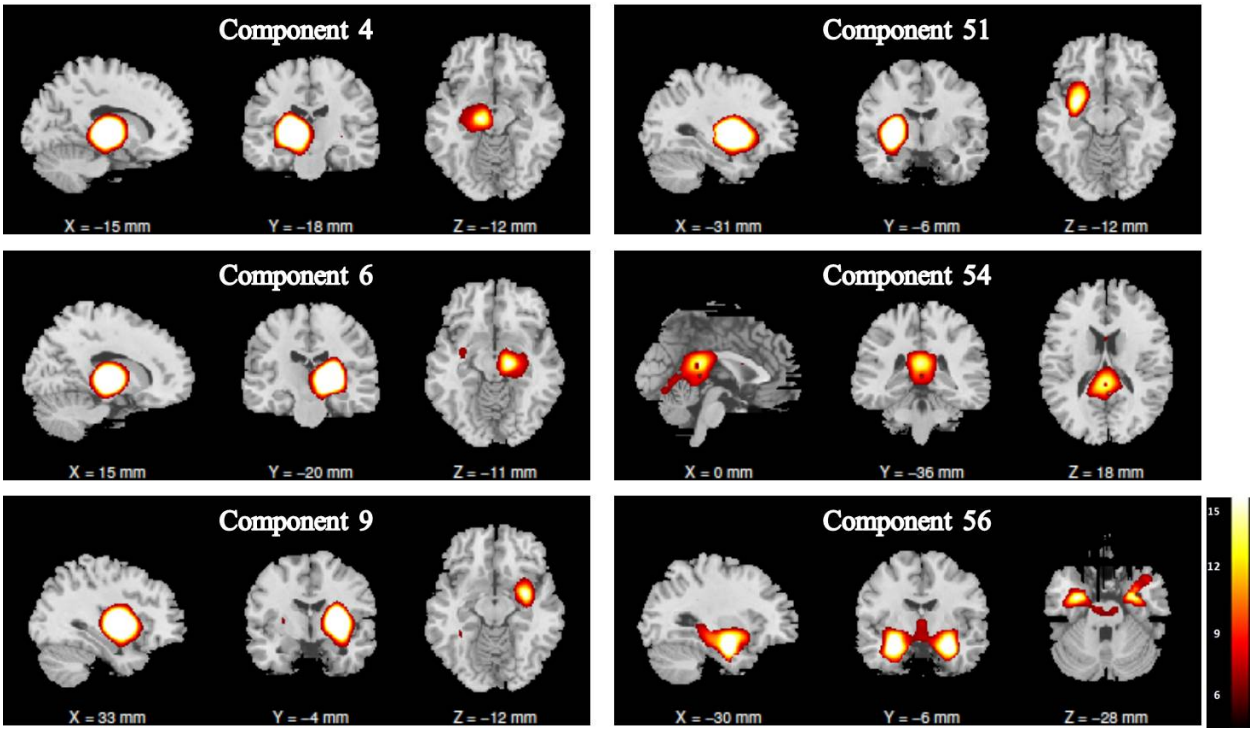

Figure S5. Spatial maps for six independent components in subcortical regions: Component 4 (thalamus); Component 6 (right thalamus and putamen); Component 9 (putamen and hippocampus); Component 51 (putamen and fusiform gyrus); Component 54 (cingulate gyrus, and superior frontal gyrus); Component 56 (amygdala, hippocampus, and striatum).

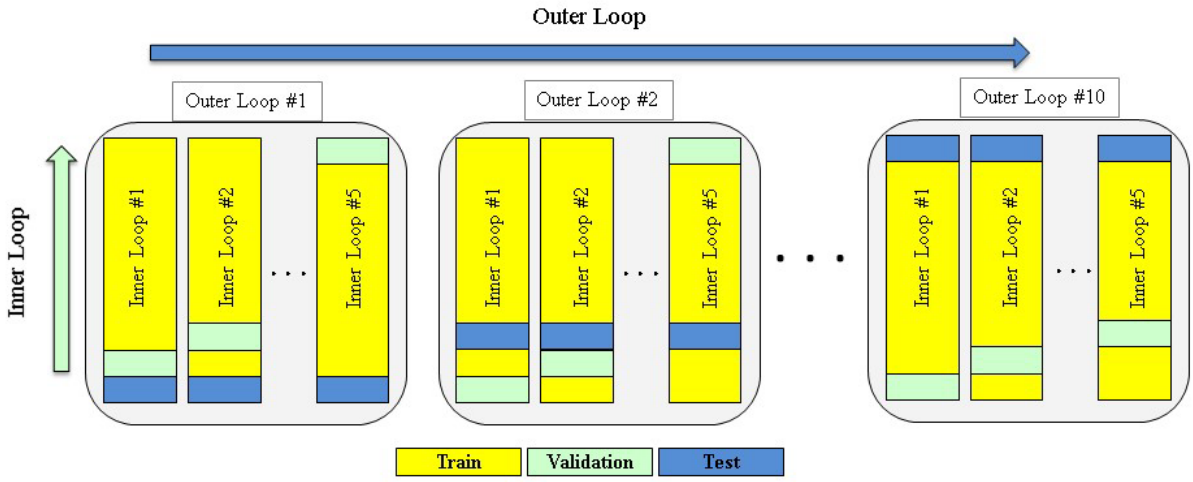

Figure S6. The nested, two-fold cross-validation method implemented in the SVM models used here. The 10-fold outer cross-validation loop was used to estimate the error on the test dataset. At each outer loop, $1/10^{th}$ of the data are set aside for testing, $1/10^{th}$ for validation and $4/5^{th}$ for training. The inner cross-validation loop was used to estimate hyperparameters of the model via grid search. At each inner loop, $1/5^{th}$ of the data are set aside for testing, $1/5^{th}$ for validation and $3/5^{th}$ for training. This model is similar to SVM models previously published from this group (40-45) with further discussion in Steele et al (40).

Supplemental References

1. Beck AT, Steer RA, Brown GK (1996): Beck Depression Inventory-II (BDI-II). San Antonio, TX: Harcourt Assessment, Inc.
2. Spielberger CD, Gorsuch RL, Lushene R, Vagg PR, Jacobs GA (1983): Manual for the State-Trait Anxiety Inventory. Palo Alto, CA: Consulting Psychologists Press.
3. Harpur TJ, Hare RD, Hakstian AR (1989): Two-factor conceptualization of psychopathy: Construct validity and assessment implications. *Psychological Assessment*. 1:6-17.
4. Hare RD (2003): *Manual for the Hare Psychopathy Checklist-Revised (2nd ed.)*. Toronto, Canada: Multi-Health Systems.
5. McConaughy EA, Prochaska JO, Velicer WG (1983): Stages of change in psychotherapy: Measuremnt and sample profiles. *Psychotherapy*. 20:368-375.
6. Wechsler D (1997): *Wechsler adult intelligence scale*. New York, NY: Psychological Corporation.
7. McLellan AT, Kushner HI, Metzger D, Peters R, Smith I, Grissom G, et al. (1992): The fifth edition of the Addiction Severity Index. *Journal of Substance Abuse Treatment*. 9:199-213.
8. Kiehl KA, Liddle PF, Hopfinger JB (2000): Error processing and the rostral anterior cingulate: An event-related fMRI study. *Psychophysiology*. 37:216-223.
9. Laaksoa MP, Vaurioc O, Koivstod E, Savolainenc L, Eronenc M, Aronenb HJ, et al. (2001): Psychopathy and the posterior hippocampus. *Behav Brain Res*. 118:187-193.
10. Friston KJ, Holmes AP, Worsley KJ, Poline J-P, Frith CD, Frackowiak RSJ (1994): Statistical parametric maps in functional imaging: A general linear approach. *Hum Brain Mapp*. 2:189-210.
11. Calhoun VD, Stevens MC, Pearlson GD, Kiehl KA (2004): fMRI analysis with the general linear model: Removal of latency-induced amplitude bias by incorporation of hemodynamic derivative terms. *Neuroimage*. 22:252-257.
12. Friston K (2002): Beyond phrenology: what can neuroimaging tell us about distributed circuitry? *Annu Rev Neurosci*. 25:221-250.
13. Biswal B, Yetkin FZ, Haughton VM, Hyde JS (1995): Functional connectivity in the motor cortex of resting human brain using echo-planar MRI. *Magn Reson Med*. 34:537-541.
14. Biswal BB, Van Kylen J, Hyde JS (1997): Simultaneous assessment of flow and BOLD signals in resting-state functional connectivity maps. *NMR Biomed*. 10:165-170.
15. Lowe MJ, Mock BJ, Sorenson JA (1998): Functional connectivity in single and multislice echoplanar imaging using resting-state fluctuations. *Neuroimage*. 7:119-132.
16. Cordes D, Haughton VM, Arfanakis K, Wendt GJ, Turski PA, Moritz CH, et al. (2000): Mapping functionally related regions of brain with functional connectivity MR imaging. *Am J Neuroradiol*. 21:1636-1644.

17. Stein T, Moritz C, Quigley M, Cordes D, Haughton V, Meyerand E (2000): Functional connectivity in the thalamus and hippocampus studied with functional MR imaging. *Am J Neuroradiol*. 21:1397-1401.

18. Cordes D, Haughton V, Carew JD, Arfanakis K, Maravilla K (2002): Hierarchical clustering to measure connectivity in fMRI resting-state data. *Magn Reson Imaging*. 20:305-317.

19. McKeown MJ, Makeig S, Brown GG, Jung TP, Kindermann SS, Bell AJ, et al. (1998): Analysis of fMRI data by blind separation into independent spatial components. *Hum Brain Mapp*. 6:160-188.

20. Calhoun VD, Adali T, Pearlson GD, Pekar JJ (2001): A method for making group inferences from functional MRI data using independent component analysis. *Hum Brain Mapp*. 14:140-151.

21. van de Ven VG, Formisano E, Prvulovic D, Roeder CH, Linden DE (2004): Functional connectivity as revealed by spatial independent component analysis of fMRI measurements during rest. *Hum Brain Mapp*. 22:165-178.

22. Esposito F, Scarabino T, Hyvarinen A, Himberg J, Formisano E, Comani S, et al. (2005): Independent component analysis of fMRI group studies by self-organizing clustering. *Neuroimage*. 25:193-205.

23. Garrity AG, Pearlson GD, McKiernan K, Lloyd D, Kiehl KA, Calhoun VD (2007): Aberrant "default mode" functional connectivity in schizophrenia. *Am J Psychiatry*. 164:450-457.

24. Calhoun VD, Liu J, Adali T (2009): A review of group ICA for fMRI data and ICA for joint inference of imaging, genetic, and ERP data. *Neuroimage*. 45:S163-S172.

25. Calhoun VD, Adali T (2012): Multisubject independent component analysis of fMRI: a decade of intrinsic networks, default mode, and neurodiagnostic discovery. *Biomedical Engineering, IEEE Reviews*. 5:60.

26. Kiviniemi V, Kantola J-H, Jauhiainen J, Hyvärinen A, Tervonen O (2003): Independent component analysis of nondeterministic fMRI signal sources. *Neuroimage*. 19:253-260.

27. Calhoun VD, Adali T, Pearlson GD, Pekar JJ (2001): Spatial and temporal independent component analysis of functional MRI data containing a pair of task-related waveforms. *Hum Brain Mapp*. 13:43-53.

28. Turner GH, Twieg DB (2005): Study of temporal stationarity and spatial consistency of fMRI noise using independent component analysis. *IEEE TRansactions on Medical Imaging*. 24:712-718.

29. Calhoun VD, Kiehl KA, Pearlson GD (2008): Modulation of temporally coherent brain networks estimated using ICA at rest and during cognitive tasks. *Hum Brain Mapp*. 29:828-838.

30. Erhardt EB, Rachakonda S, Bedrick EJ, Allen EA, Adali T, Calhoun VD (2011): Comparison of multi-subject ICA methods for analysis of fMRI data. *Hum Brain Mapp*. 32:2075-2095.

31. Kiviniemi V, Starck T, Remes J, Long X, Nikkinen J, Haapea M, et al. (2009): Functional segmentation of the brain cortex using high model order group PICA. *Hum Brain Mapp*. 30:3865-3886.

32. Abou-Elseoud A, Starck T, Remes J, Nikkinen J, Tervonen O, Kiviniemi V (2010): The effect of model order selection in group PICA. *Hum Brain Mapp*. 31:1207-1216.

33. Ystad M, Eichele T, Lundervold AJ, Lundervold A (2010): Subcortical functional connectivity and verbal episodic memory in healthy elderly--a resting state fMRI study. *Neuroimage*. 52:379-388.

34. Allen EA, Erhardt EB, Damaraju E, Gruner W, Segall JM, Silva RF, et al. (2011): A baseline for the multivariate comparison of resting-state networks. *Front Syst Neurosci*. 5:1-23.

35. Bellemann ME, Spitzer M, Brix G, Kammer T, Loose R, Schwartz A, et al. (1995): Neurofunctional MRI imaging of higher cogntive performance of the human brain. *Radiologe*. 35:272-282.

36. Jafri MJ, Pearlson GD, Stevens M, Calhoun VD (2008): A method for functional network connectivity among spatially independent resting-state components in schizophrenia. *Neuroimage*. 39:1666-1681.

37. Meyer PE, Bontempi G (2006): On the Use of Variable Complementarity for Feature Selection in Cancer Classification. *Applications of Evolutionary Computing*. Berlin: Sprnger Berlin Heidelberg, pp 91-102.

38. Benjamini Y, Hockberg Y (1995): Controlling the false discovery rate: A practical and powerful approach to multiple testing. *Journal of the Royal Statistical Society*. 57:289-300.

39. Yekutieli D, Benjamini Y (1997): Resampling-based false discovery rate controlling multiple test procedures for correlated test statistics. *Journal of Statistical Planning and Inference*. 82:171-196.

40. Steele VR, Fink BC, Maurer JM, Arbabshirani MR, Wilber CH, Jaffe AJ, et al. (2014): Brain potentials measured during a Go/NoGo task predict completion of substance abuse treatment. *Biol Psychiatry*. 76:75-83.

41. Steele VR, Claus ED, Aharoni E, Vincent GM, Calhoun VD, Kiehl KA (2015): Multimodal imaging measures predict rearrest. *Front Hum Neurosci*. 9:425.

42. Cope LM, Ermer E, Gaudet LM, Steele VR, Eckhardt AL, Arbabshirani MR, et al. (2014): Abnormal brain structure in youth who commit homicide. *NeuroImage: Clinical*. 4:800-807.

43. Fink BC, Steele VR, Maurer JM, Fede SJ, Calhoun VD, Kiehl KA (2016): Brain potentials predict substance abuse treatment completion in a prison sample. *Brain and Behavior*. 6:1-14.

44. Steele VR, Rao V, Calhoun VD, Kiehl KA (2017): Machine learning of structural magnetic resonance imaging predicts psychopathic traits in adolescent offenders. *Neuroimage*. 145:265-273.

45. Kiehl KA, Anderson NE, Aharoni E, Maurer JM, Rao V, Koenigs M, et al. (*under review*): Age of gray matters: Neuroprediction of recidivism.